Noname manuscript No.
(will be inserted by the editor)

New Look on Relay Selection Strategies for Full-Duplex Multiple-Relay NOMA over Nakagami-m Fading Channels

Tu-Trinh Thi Nguyen[1], Dinh-Thuan Do[2,*], Yeong-Chin Chen [2], Chakchai So-In [3], Md. Arafatur Rahman[4]

Received: date / Accepted: date

Abstract By removing the orthogonal use of radio-resources, non-orthogonal multiple access (NOMA) has been introduced to improve the spectral efficiency of fifth generation (5G) and beyond networks. This paper studies the system performance in a dual-hop multi-relay NOMA using decode-and-forward (DF) scheme over Nakagami-m fading channels. A group of NOMA users is considered, i.e. the near and far users which are decided by how strong these related channels are. Specifically, we obtain a closed-form expression of the outage probability of the near/far NOMA users when the several relay selection schemes are adopted for selecting the best among M intermediate relays. As main finding, this paper introduces three strategies including two-stage relay selection, max-min and power allocation based relay selection schemes. As main benefit, the NOMA users are considered to employ selection combining technique in order to improve signal transmissions for an increased reliability in the context of massive connections in 5G wireless communications. By conducting numerical simulations, we evaluate the impact of the number of

Tu-Trinh Thi Nguyen
Faculty of Electronics Technology, Industrial University of Ho Chi Minh City (IUH), Ho Chi Minh City, Vietnam
E-mail: nguyenthitutrinh@iuh.edu.vn

Chakchai So-In
Applied Network Technology Laboratory Department of Computer Science, Faculty of Science, Khon Kaen University, Khon Kaen 40002, Thailand
E-mail: chakso@kku.ac.th

MD. Arafatur Rahman
School of Mathematics and Computer Science, University of Wolverhampton, WV1 1LY Wolverhampton, United Kingdom
E-mail: arafatur.rahman@wlv.ac.uk
*Corresponding author: Dinh-Thuan Do
Dinh-Thuan Do, Yeong-Chin Chen, Department of Computer Science and Information Engineering, College of Information and Electrical Engineering,
Asia University, Taichung 41354, Taiwan.
E-mail: dodinhthuan@asia.edu.tw; ycchenster@asia.edu.tw

intermediate relays, the NOMA power allocation factor, and the Nakagami-m fading severity parameter on the outage performance of the NOMA users. Finally, the outage probability along with throughout in delay-limited transmission mode are provided via numerical results and the necessary comparisons are provided.

Keywords Non-orthogonal multiple access (NOMA) · outage probability · relay selection.

1 Introduction

Due to potential in achieving high spectral efficiency (SE), Non-orthogonal multiple access (NOMA) is recognized as promising multiple access scheme to implement the fifth generation (5G) mobile networks [1], [2]. Fortunately, cooperative communications can be combined with NOMA to form cooperative NOMA and the effect of fading can be mitigated and a higher diversity order can be obtained accordingly [1]. In the open literature, several proposed system models of cooperative relaying NOMA are introduced. In [3], to enhance the reliable transmission to far users, strong users with better channel conditions serves as relays. the decode-and-forward (DF) and amplify-and-forward (AF) protocols are considered to support transmission from base station (BS) to the paired users through a dedicated relay as works in [4], [5]. In [6], it was assumed that a shared AF relay is required by two sources can simultaneous signal transfer to their targeted destinations using the same frequency. To increase the system performance of the waek users with worse channel conditions, the switching scheme between cooperative NOMA and orthogonal multiple access (OMA) is recommended in [7]. It can be seen such a interesting trend as combining advantages of wireless power transfer technique in NOMA to form wireless powered NOMA network [8]-[10]. The authors in [8] introduced a novel EH protocol based on time power switching-based relaying (TPSR) architecture to implement NOMA together with amplify-and-forward (AF) relaying mode. NOMA in scenario of the deployment of simultaneous wireless information and power transfer (SWIPT) is considered degradation performance under the influence of intercell interference (ICI) [9]. They examined on the system outage behavior with important derived results to provide guidelines in design of NOMA. To implement device-to-device (D2D) communication, cooperative NOMA network is investigated in [10]. In such D2D NOMA, to serve NOMA far user two relaying modes are studied. Particularly, Amplify and Forward (AF) and Decode and Forward (DF) mode are implemented to provide signal processing at relay. The authors in [11] evaluated impact of imperfect channel state (CSI) information in an energy harvesting (EH) cooperative non-orthogonal multiple access (NOMA) network, and this system model includes a source, two users, and an EH relay.

When cooperative NOMA benefits from multiple relays, to control the system complexity relay selection (RS) has to be properly designed while the full diversity order still archieved [12–14]. The two-stage max-min RS ssytem

containing a relay which was selected to put effort to serve the high-rate user using proposed a fixed power allocation (PA) scheme as in [12]. They shown that at such sytem with the low rate user was still satisfied in term of the quality of service (QoS) requirement. Further, the PA fractions were controled according to the instantaneous channel state information (ICSI) to form dynamic PA based two-stage RS scheme in [13]. The authors in [14] introduced a two-stage max weighted-harmonic-mean (MWHM) RS scheme and a two-stage weighted-maxmin (WMM) RS scheme and such a cooperative NOMA benefits form both dynamic PA and fixed PA schemes. The authors in [14] considered the user ordering strategies designed according to the ICSI suitable for all the users satisfying an identical priority. The achievable outage probability can be achieved from the simulation results regarding the two-stage MWHM RS scheme [14] is lower than the RS schemes in [12], [13]. Reported as common results in [14], [15], the low-rate user not only had a higher priority, but also was ordered before the high-rate user and it is resulted from the users ordered by their QoS requirements (i.e., service priorities). The authors in [15] introduced an Internet-of-Things (IoT) system containing a relay selection to deploy NOMA architecture. In particular, this paper exhibited a new scheme to consider secure performance in such a relay selection enabled NOMA.

To improve the coverage of 5G networks, opportunistic relay selection (ORS) relaying [16], [17] and buffer-aided relaying [18], [19] are of crucial importance techniques among relay selection schemes implemented in relaying networks. In addition, buffer-aided and ORS provide the lower outage probability of the network, and it is best fit to apply in delay-tolerant systems. In addition, hybrid relay selection (HRS) based on the max-max relay selection (MMRS) is proposed in [20] proposed. In this papr, one time-slot to two relays is allocated in transmission links including the strongest source-relay and relay-destination links. Different with [20], by allocating each time-slot to either an relay-destination or an source-relay transmission, MMRS/max link algorithm with adaptive link selection was proposed in [21] to exhibit enhanced diversity. The authors in [22] presented a hybrid MMRS/max link algorithm. By prioritizing relay-destination transmissions and/or considering buffer state information (BSI) for relay selection, delay-aware schemes are detailed introduced in [23]-[28]. Furthermore, thresholds are acquired at the buffers to further enhance the diversity of buffer aided relaying, and the number of packets, activating relays further satisfy those thresholds [29], [30].

1.1 Related Work

Different from popular applications of half-duplex (HD), by permitting the radios to simultaneously transmit and receive on the same frequency channel full-duplex (FD) scheme contributes to improve the spectral efficiency. Due to signal leakage, the self-interference exists as the main challenge for realizing full-duplex communication, and hence the performance gain achieved by FD architecture significantly degrades as in [31]. Fortunately, FD communi-

cations have been successfully deployed thanks to using analog and digital self-interference cancellation schemes [32]. The author in [33] considered orthogonal frequency division multiplexing systems in term of rate region of FD links. In [34], the authors studied power-domain NOMA scheme to send information from the base station to the destinations, and partial relay selection is adopted to decide the relay using the channel state information achieved in the first hop. The authors characterized performance by examining both the outage probability and the ergodic capacity. In addition, they derived closed-form expressions in lower-bound, approximate, and asymptotic analyses to reduce the complexity in computation. Reference [35] presented three approaches to support device-to-device mode in NOMA systems, namely non-energy harvesting relaying (Non-EHR), energy harvesting relaying (EHR) and quantize-map-forward relaying (QMFR) schemes. While the buffer-aided (BA) FD NOMA relaying was proposed to improve the spectral efficiency of a single-source two-user network [36]. They employed opportunistic relay selection by activating one or two FD relays to support the end-to-end communication [36].

1.2 Our contributions

However, a general case of efficient relay selection in downlink of NOMA network needs more research. This motivate us to study more methods of relay selection to improve the performance. In particular, we have new look on performance of FD relaying system with general channel model, i.e. Nakagami-m fading channel along with three specific relay selection schemes which has not been studied yet. Different from Rayleigh fading reported in most of studies regarding relay selection strategy, it is necessary to further system performance of relay selection aided NOMA system under other fading conditions. To characterize small-scale fading in wireless communications, other more complex but more general models for are Rician or Nakagami-m distributions. The main reason to study these distributions since they take into account the light-of-sight (LoS) components. Considering the case of Nakagami-m fading, individual multi-path components with very similar time delay are modeled by the Nakagami-m distribution, i.e. m represents the fading severity. Comparing to NOMA relay selection schemes using Rayleigh fading [6], [12], once can find difficult to compute outage probability in the case of Nakagami-m fading. In particular, higher m means a higher possibility of having LoS communications. In general, we provide main difference between our paper and related studies, shown in Table 1. Our contributions can be summarized as follows

- Although the conventional max-min relay selection (MM) and two-stage RS (TSRS) strategies carried out in the literature for NOMA system [12], we extend to more complicated scenario by enabling FD scheme at relays. In this paper, two mentioned schemes are implemented and such TSRS is adopted for FD transmission in RS-NOMA mode but also suggest the new power allocation based RS strategy (PA).

Table 1 COMPARISON WITH RELATED STUDIES.

Reference	Fading				PA	RS		
	Rayleigh	Nakagami-m	FD	HD			AF	DF
[5]		•		•			•	
[6]	•			•			•	
[12]	•			•		•		
[13]	•			•	•	•	•	•
[14]	•			•	•	•		•
This paper		•	•		•	•		•

– We derive closed-form expressions of outage probability for three strategies (MM, TSRS, and PA). It is obvious that the number of relay makes main influence on outage performance. Depending demand and efficiency, we decide which RS is suitable to implement RS-NOMA system.
– We performance numerical simulations to verify and recommend PA selected to implement RS-NOMA in particular requirement of quality of service.

1.3 Structure of paper

The structure of this paper is as follows. Section II presents the system model and preliminaries, necessary for the development of our results. Section III provides the process for two stages RS. Then, Section IV gives in detail max-min relay selection algorithm, while the case of power allocation based RS scheme is presented in Section V. Theoretical analysis of the proposed algorithms is given in the corresponding section. In Section VI, we present a performance evaluation in term of outage behavior and, finally, in Section VII, conclusion remarks are provided and possible future directions are highlighted.

Notation: $f_Z(.)$ and $F_Z(.)$ represent the probability distribution function (PDF) and the cumulative distribution function of random variables (RVs), Z, respectively. $\Pr(.)$ *is the outage probability function and* $E\{.\}$ *indicates the expectation.*

2 SYSTEM MODEL AND SIGNAL MODELING

Channel assumption: It is assumed that all channel gains undergo independence Nakagami-m fading distribution. The PDF and CDF are given respectively by [40]

$$f_{|z|^2}(x) = \frac{x^{m_z-1}}{\Gamma(m_z)\beta_z^{m_z}} \mathrm{e}^{-\frac{x}{\beta_z}}, \tag{1}$$

$$\begin{aligned} F_{|z|^2}(x) =& 1 - \frac{1}{\Gamma(m_z)} \Gamma\left(m_z, \frac{x}{\beta_z}\right) \Bigg(\\ =& 1 - \mathrm{e}^{-\frac{x}{\beta_z}} \sum_{n=0}^{m_z-1} \frac{x^n}{n!\beta_z^n}, \end{aligned} \tag{2}$$

where $\beta_z \triangleq \lambda_z/m_z$ with λ_z and m_z represent the channel mean power (for example: $\lambda_{h_b} = \mathrm{E}\left\{|h_b|^2\right\}$) and integer fading factor. $\Gamma(.)$ is the gamma function. x is a variable.

2.1 Topology network

This paper considers NOMA scheme to implement cooperative mode and relay selection in downlink. As depicted in Fig. 1, a base station (BS) conveys data messages throughout downlink channels toward the first destination D_1 and the second destination D_2 through a relay (R) from the M available relays. These nodes are denoted by D_1 and D_2 respectively. In this scenario, there is no direct links between the BS and destinations due to obstacle or deep fading, thus the relay selection scheme provides advantage for such communication transmission, denoted by $\mathcal{S}_{\mathcal{R}} = \{r_k, k = 1, \ldots, M\}$. It is further assumed a flat block-fading model is adopted and these fading channels on the links is statistically independent and follow the Nakagami-m distribution. The BS is benefited by several relay selection schemes to enable one of the M relays to transfer its message to D_1 and D_2. In this paper, the comparison of these selection relay scheme is also considered.

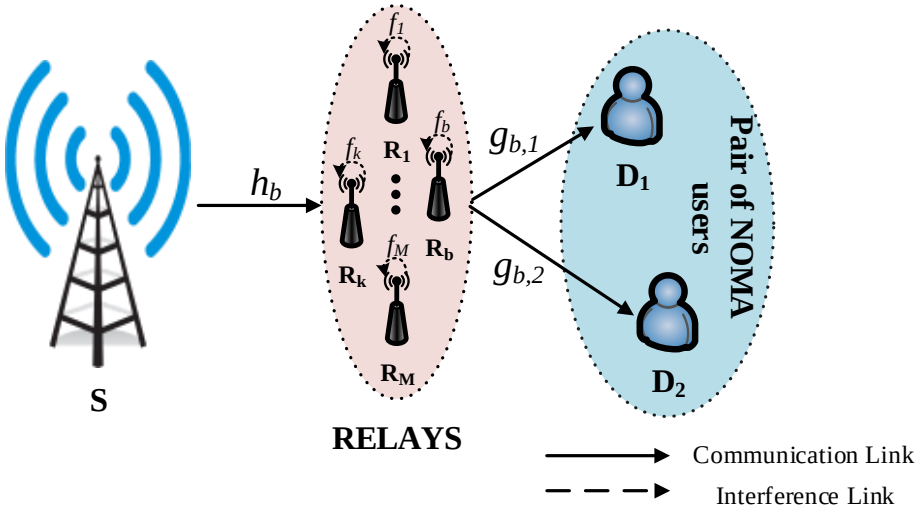

Fig. 1 System model of NOMA with various relay selection modes.

2.2 Signal Model

We can describe the details of three proposed RS schemes as below. Considering the structure of transmission block time, we design two phases including RS and information transmission (IT) phases. To select the best relay for data forwarding, the system acquires RS phase. In perspective of two-stage transmission, the first stage of such RS is to ensure that the user D_1's targeted data rate is satisfied, and the second of such RS is to maximize the user D_2's rate opportunistically. After this important phase, the considered system employs rest of block time to information processing, so-called information transmission (IT) phase [12].

In the IT phase, the source transmits the superimposed symbol $x = \sqrt{\upsilon_1}x_1 + \sqrt{\upsilon_2}x_2$, with x_1, x_2 are the signal for D_1, D_2 and $\upsilon_1 \geq \upsilon_2$, $\upsilon_1 + \upsilon_2 = 1$ due to more priority access of D_1 than that of D_2. The transmit power is assumed $\mathrm{P_s}$ for source and identically $\mathrm{P_r}$ for all relay. All channel coefficients undergo Nakagami-m fading environment with integer m value. We denote channel factors from link from S to k-th relay and self-interference (SI) link at each relay h_k and f_k, respectively. The received signal at relay k-th can be expressed as below

$$\begin{aligned} y_{r_k} =& P_s h_k x + P_r f_k \hat{x}_{r_k} + n_{r_k} \\ =& P_s h_k \left(\sqrt{\upsilon_1}x_1 + \sqrt{\upsilon_2}x_2\right) + P_r f_k \hat{x}_{r_k} + n_{r_k}, \end{aligned} \tag{3}$$

where $\hat{x}_{r_k} = \sqrt{\upsilon_1}\hat{x}_1 + \sqrt{\upsilon_2}\hat{x}_2$ is the symbol transmitted at relay with $\hat{x}_1$, $\hat{x}_2$ are the re-encoded symbols with zero mean and unit variance, n_{r_k} denotes the additive white Gaussian noise (AWGN) with zero mean and variance σ^2. Based on the NOMA principle, the relay first retrieves D_1's data by treating D_2's signal as interference. Secondly, the relay removes the D_1's signal and discovers D_2's data. Therefore, the signal to interference plus noise ratio (SINR) to detect x_1 at relay k-th can be formulated by

$$\gamma_{r_k \leftarrow 1} = \frac{\upsilon_1 \rho_s |h_k|^2}{\upsilon_2 \rho_s |h_k|^2 + \rho_r |f_k|^2 + 1}. \tag{4}$$

The SINR at relay node to decode the second user's signal is given by

$$\gamma_{r_k \leftarrow 2} = \frac{\upsilon_2 \rho_s |h_k|^2}{\rho_r |f_k|^2 + 1}, \tag{5}$$

where $\rho_s \triangleq \mathrm{P}_s/\sigma_0^2$ and $\rho_r \triangleq \mathrm{P}_r/\sigma_0^2$ are transmission SNR of source and relay node, respectively. Simultaneously, relay forwards signal to destination based on DF protocol. Thus, the received signals at user D_1 and D_2 throughout relay k are given respectively

$$\begin{aligned} y_{\mathrm{D}_1} =& \mathrm{P_r} g_{k,1} \hat{x}_{r_k} + n_{d_1} \\ =& \mathrm{P_r} g_{k,1} \left(\sqrt{\upsilon_1}\hat{x}_1 + \sqrt{\upsilon_2}\hat{x}_2\right) + n_{d_1}, \end{aligned} \tag{6}$$

and

$$\begin{aligned} y_{\mathrm{D}_2} =& \mathrm{P_r} g_{k,2} \hat{x}_{r_k} + n_{d_2} \\ =& \mathrm{P_r} g_{k,2} \left(\sqrt{\upsilon_1}\hat{x}_1 + \sqrt{\upsilon_2}\hat{x}_2\right) + n_{d_2}. \end{aligned} \tag{7}$$

where n_{d_1}, n_{d_2} denote the (AWGN), $g_{k,1}$, $g_{k,2}$ are the channel coefficient from the k-th relay to D_1, D_2.

According to early assumption, D_1 is a priority device and thus be allocated more power. As a result, D_1 can directly decode its data by dealing with D_2's signal as interference. Hence, the SINR at D_1 in order to decode its own data can be written by

$$\gamma_{\mathrm{D}_1} = \frac{\upsilon_1 \rho_r |g_{k,1}|^2}{\upsilon_2 \rho_r |g_{k,1}|^2 + 1}. \tag{8}$$

Additionally, D_2 only recovers its data after successfully decompositing user 1 data and applying SIC. Then, the SINR and SNR at second user D_2, to detect the first user symbol for SIC purpose and to discover its own data are respectively given by

$$\gamma_{\mathrm{D}_2 \leftarrow 1} = \frac{\upsilon_1 \rho_r |g_{k,2}|^2}{\upsilon_2 \rho_r |g_{k,2}|^2 + 1}, \tag{9}$$

and

$$\gamma_{\mathrm{D}_2} = \upsilon_2 \rho_r |g_{k,2}|^2. \tag{10}$$

2.3 Instantaneous channel capacity

At k-th relay, the achievable instantaneous rates correspond to the first user and the second user are given respectively as

$$\begin{aligned} C_{r_k}^1 =& \log_2 \left(1 + \gamma_{r_k \leftarrow 1}\right) \\ =& \log_2 \quad 1 + \frac{\upsilon_1 \rho_s |h_k|^2}{\upsilon_2 \rho_s |h_k|^2 + \rho_r |f_k|^2 + 1} \Bigg) \Bigg(\end{aligned} \tag{11}$$

and

$$\begin{aligned} C_{r_k}^2 =& \log_2 \left(1 + \gamma_{r_k \leftarrow 2}\right) \\ =& \log_2 \quad 1 + \frac{\upsilon_2 \rho_s |h_k|^2}{\rho_r |f_k|^2 + 1} \Bigg) \Bigg(\end{aligned} \tag{12}$$

Besides, the data rate accomplished at user D_1 is given by

$$\begin{aligned} C_{r_k, \mathrm{D}_1} =& \log_2 \left(1 + \gamma_{d_1}\right) \\ =& \log_2 \quad 1 + \frac{\upsilon_1 \rho_r |g_{k,1}|^2}{\upsilon_2 \rho_r |g_{k,1}|^2 + 1} \Bigg) \Bigg(\end{aligned} \tag{13}$$

We continue to examine the achievable data rates for the first user's signal and the second user 2's signal are respectively as

$$\begin{aligned} C_{r_k, \mathrm{D}_2}^1 =& \log_2 \left(1 + \gamma_{r_k, \mathrm{D}_2 \leftarrow 1}\right) \\ =& \log_2 \quad 1 + \frac{\upsilon_1 \rho_r |g_{k,2}|^2}{\upsilon_2 \rho_r |g_{k,2}|^2 + 1} \Bigg) \Bigg(\end{aligned} \tag{14}$$

and

$$\begin{aligned} C_{r_k,\mathrm{D}_2} =& \log_2\left(1+\gamma_{r_k,d_2}\right) \\ =& \log_2\left(1+\upsilon_2\rho_r|g_{k,2}|^2\right) \end{aligned} \tag{15}$$

We continue to examine performance of two strategies, i.e. MM, PA and TSRS in the next section. To conduct explicit procedures to determine best relay, the consideblack system need CSI information feedback to the source to transmit signal to dedicated relay before forwarding to destination. Such mechanism further require overhead transmission to estimate CSI at receivers. In practical situation, due to delays generated by the feedback mechanism, the CSI associated nodes might be different from the actual one. More specifically, CSI may be outdated, the system may meet degrading performance. The deployment of three schemes depends on how we trust on the feedback information back to the BS. However, we could consider details in the future work.

3 Max-Min Relay Selection (MM)

This subsection presents traditional MM scheme which minimizes system outage performance. Before having further computation, we consider following lemma.

Lemma 1: We define a function which is used throughout paper as below

$$\begin{aligned} \Phi\left(a,b,k\right) \triangleq& \Pr\left(a|h_k|^2 \geq b|f_k|^2+1\right) \\ =& \frac{\mathrm{e}^{\frac{-1}{a\beta_h}}}{\Gamma\left(m_f\right)\beta_f^{m_f}} \sum_{n=0}^{m_h-1}\sum_{k=0}^{n}\binom{n}{k}\left(\frac{1}{\beta_h^n a^n}\frac{\Gamma\left(k+m_f\right)b^k}{n!}\left(\frac{1}{\beta_f}+\frac{b}{a\beta_h}\right)^{-k-m_f}\right. \end{aligned}. \tag{16}$$

Proof: See in Appendix A.

We call R_1^{th} and R_2^{th} as target rates for D_1 and D_2, respectively. The partial outage probability of the considered NOMA system with the help of k-th relay is expressed as

$$\begin{aligned} OP_k =& \Pr\left(\frac{C_{r_k}^1}{R_1^{\mathrm{th}}}<1\cup\frac{C_{r_k,d_1}}{R_1^{\mathrm{th}}}<1\cup\frac{C_{r_k,d_2}^1}{R_1^{\mathrm{th}}}<1\cup\frac{C_{r_k}^2}{R_2^{\mathrm{th}}}<1\cup\frac{C_{r_k,d_2}}{R_2^{\mathrm{th}}}<1\right) \\ =& 1-\Pr\left(\min\left(\frac{C_{r_k}^1}{R_1^{\mathrm{th}}},\frac{C_{r_k,d_1}}{R_1^{\mathrm{th}}},\frac{C_{r_k,d_2}^1}{R_1^{\mathrm{th}}},\frac{C_{r_k}^2}{R_2^{\mathrm{th}}},\frac{C_{r_k,d_2}}{R_2^{\mathrm{th}}}\right)\geq 1\right) \end{aligned} \tag{17}$$

In order to minimize whole system outage probability, i.e. $\min\limits_{k\in\mathcal{S}_\mathcal{R}}\left(OP\right)$, the index of selected relay in MM scheme is formulated by

$$b_{MM} = \arg\max_{k\in\mathcal{S}_\mathcal{R}}\left(\min\left(\frac{\gamma_{r_k\leftarrow 1}}{\delta_1^{\mathrm{th}}},\frac{\gamma_{r_k,d_1}}{\delta_1^{\mathrm{th}}},\frac{\gamma_{r_k,d_2\leftarrow 1}}{\delta_1^{\mathrm{th}}},\frac{\gamma_{r_k\leftarrow 2}}{\delta_2^{\mathrm{th}}},\frac{\gamma_{r_k,d_2}}{\delta_2^{\mathrm{th}}}\right)\right) \tag{18}$$

where $\delta_1^{\text{th}} = 2^{R_1^{\text{th}}} - 1$, $\delta_2^{\text{th}} = 2^{R_2^{\text{th}}} - 1$.
Since the channels are independent with each other, the outage probability of system can be determined as the following proposition.
Proposition 1: The outage performance of NOMA system relying on MM scheme is given by

$$OP_{MM} = \prod_{k=1}^{M} OP_k, \tag{19}$$

in which, OP_k is given by

$$OP_k \triangleq 1 - \Phi\left(\varphi_1\rho_s, \rho_r\right) F_{|g_{k,1}|^2}\left(\frac{1}{\omega_1\rho_r}\right) F_{|g_{k,2}|^2}\left(\frac{1}{\varphi_1\rho_r}\right) \tag{20}$$

with $\omega_1 \triangleq \frac{\upsilon_1}{\delta_1^{\text{th}}} - \upsilon_2$ and $\varphi_1 \triangleq \min\left(\omega_1, \frac{\upsilon_2}{\delta_2^{\text{th}}}\right)$, while Φ and F functions are defined in Lemma and (2) respectively.

Proof: See in Appendix B.
It is noted that, in case of $\omega_1 \leq 0$ the outage is equal one, i.e. $OP_k = 1$.

4 Two-stage Relay Selection (TSRS)

In this research, we adopt the relay selection (RS) strategy proposed in [13], however this TSRS scheme is consideblack for FD relaying transmission. This section provides derivative analysis of the closed-form expressions of the outage probability at with TSRS scheme.
As recent work [13], it can be obtained the subset of relay which can support to successfully transmit user 1 data for relay, D_1 and D_2. This set can be mathematically formulated as below [13]

$$\mathcal{B}_{\mathcal{R}} = \left\{ r_\ell : r_\ell \in \mathcal{S}_{\mathcal{R}}, C_{r_\ell}^1 \geq R_1^{\text{th}}, C_{r_\ell,d_1} \geq R_1^{\text{th}}, C_{r_\ell,d_2}^1 \geq R_1^{\text{th}} \right. \tag{21}$$

The best relay is chosen by the following criterion

$$b = \arg\max_{i \in \mathcal{B}_{\mathcal{R}}} \left\{ \min\left(C_{r_i}^2, C_{r_i,d_2}\right) \right\} \tag{22}$$

Based on the TSRS principle, the overall system outage probability is given by [39]

$$OP_{TSRS} = \Pr\left(\mathcal{B}_{\mathcal{R}} = \emptyset\right) + \Pr\left(\min\left(C_{r_b}^2, C_{r_b,d_2}\right) < R_2^{\text{th}} : \mathcal{B}_{\mathcal{R}} \neq \emptyset\right) \tag{23}$$

We consider the first element in (23) *as below.*

Defining Ω_ℓ as the probability that the relay r_ℓ is in the active relay set $\mathcal{B}_\mathcal{R}$, the Ω_ℓ can be mathematically formulated as

$$\begin{aligned}\Omega_\ell &\triangleq \Pr\left(r_\ell \in \mathcal{B}_\mathcal{R}\right)\\ &= \Pr\left(C^1_{r_\ell} \geq R_1^{\text{th}}, C_{r_\ell,d_1} \geq R_1^{\text{th}}, C^1_{r_\ell,d_2} \geq R_1^{\text{th}}\right)\end{aligned} \tag{24}$$

According to the independence of channel assumptions, the first term of right hand side in (23) can be determined as

$$\begin{aligned}\Pr\left(\mathcal{B}_\mathcal{R} = \emptyset\right) &= \prod_{\ell=1}^{M}\left(1-\Omega_\ell\right)\\ &= (1-\Omega_\ell)^M.\end{aligned} \tag{25}$$

With probability reported in (24), such probability can be computed as (26), shown below, where $\omega_1 \triangleq \frac{\upsilon_1}{\delta_1^{\text{th}}} - \upsilon_2$.

$$\begin{aligned}\Omega_\ell =& \Pr\left(C_{r_\ell \leftarrow 1} \geq R_1^{\text{th}}\right)\Pr\left(C_{r_\ell,d_1} \geq R_1^{\text{th}}\right)\Pr\left(C^1_{r_\ell,d_2} \geq R_1^{\text{th}}\right)\\ =& \Pr\left(\frac{\upsilon_1\rho_s|h_\ell|^2}{\upsilon_2\rho_s|h_\ell|^2+\rho_r|f_\ell|^2+1} \geq \delta_1^{\text{th}}\right)\Pr\left(\frac{\upsilon_1\rho_r|g_{\ell,1}|^2}{\upsilon_2\rho_r|g_{\ell,1}|^2+1} \geq \delta_1^{\text{th}}\right)\\ &\times \Pr\left(\frac{\upsilon_1\rho_r|g_{\ell,2}|^2}{\upsilon_2\rho_r|g_{\ell,2}|^2+1} \geq \delta_1^{\text{th}}\right)\\ =& \Phi\left(\omega_1\rho_s, \rho_r, \ell\right) \times \left[1 - F_{|g_{\ell,1}|^2}\left(\frac{1}{\omega_1\rho_r}\right)\right] \times \left[1 - F_{|g_{\ell,2}|^2}\left(\frac{1}{\omega_1\rho_r}\right)\right]\end{aligned} \tag{26}$$

We consider the second element in (23) *as below.*

Particularly, the second component in (23) is computed by [39]

$$OP_{TSRS,2} = \sum_{t=1}^{M}\Pr\left(|B_R| = t\right) \times \Pr\left(\min\left(C^2_{r_b}, C_{r_b,d_2}\right) < R_2^{\text{th}}, |B_R| = t\right) \tag{27}$$

According to the optimal relay selection manner in (22) and independence of channel assumptions, equation (27) can be further computed as (28), shown as below.

$$\begin{aligned}OP_{TSRS,2} &= \sum_{t=1}^{M}\Pr\left(\max_{k\in\mathcal{B}_\mathcal{R}}\min\left(C^2_{r_k}, C_{r_k,d_2}\right) < R_2^{\text{th}}, |\mathcal{B}_\mathcal{R}| = t\right)\Pr\left(|\mathcal{B}_\mathcal{R}| = t\right)\\ &= \sum_{t=1}^{M}\prod_{k=1}^{t}\Pr\left(\min\left(C^2_{r_k}, C_{r_k,d_2}\right) < R_2^{\text{th}}, |\mathcal{B}_\mathcal{R}| \neq \emptyset\right)\Pr\left(|\mathcal{B}_\mathcal{R}| = t\right).\end{aligned} \tag{28}$$

Firstly, we determine the term in (28) as follow. In the event of arbitrary relay selection, this outage probability can be determined by

$$\begin{aligned}\Xi_k =& \Pr\left(\min\left(C^2_{r_k}, C_{r_k,d_2}\right) < R_2^{\text{th}} : k \in \mathcal{B}_\mathcal{R}, |\mathcal{B}_\mathcal{R}| \neq \emptyset\right)\\ =& 1 - \frac{\Pr\left(C^2_{r_k} \geq R_2^{\text{th}}, C_{r_k,d_2} \geq R_2^{\text{th}}, C^1_{r_k} \geq R_1^{\text{th}}, C_{r_k,d_1} \geq R_1^{\text{th}}, C^1_{r_k,d_2} \geq R_1^{\text{th}}\right)}{\Pr\left(k \in \mathcal{B}_\mathcal{R}\right)}\\ =& 1 - \frac{\Xi_{k,1}}{\Pr\left(k \in \mathcal{B}_\mathcal{R}\right)},\end{aligned} \tag{29}$$

with $\Pr\left(k \in \mathcal{B}_\mathcal{R}\right) = \Omega_k$ and by following simple procedure, we can obtain

$$\Xi_{k,1} = \Phi\left(\varphi_1\rho_s, \rho_r, k\right)\left[1 - F_{|g_{k,1}|^2}\left(\frac{1}{\omega_1\rho_r}\right)\right] \times \left[1 - F_{|g_{k,2}|^2}\left(\frac{1}{\varphi_1\rho_r}\right)\right], \tag{30}$$

where $\varphi_1 \triangleq \min\left(\frac{\upsilon_2}{\delta_2^{\text{th}}}, \omega_1\right)$. Secondly, the value of term $\Pr\left(|\mathcal{B}_\mathcal{R}| = t\right)$ in (28) is computed as

$$\Pr\left(|\mathcal{B}_\mathcal{R}| = t\right) = \binom{M}{t} \prod_{n=1}^{M-t} \Pr\left(\pi(n) \in \mathcal{B}_\mathcal{R}\right) \prod_{k=M-t+1}^{M} \Pr\left(\pi(k) \notin \mathcal{B}_\mathcal{R}\right), \tag{31}$$

where $\pi\left(\bullet\right)$ represents a arbitrary permutation of the relays. By applying the same steps in (23), we can yield

$$\Pr\left(|\mathcal{B}_\mathcal{R}| = t\right) = \binom{M}{t} \left(\Omega_\ell\right)^t \left(1 - \Omega_\ell\right)^{M-t} \tag{32}$$

Proposition 2: The outage probability and the throughput with TSRS protocol are expressed by

$$OP_{TSRS} = \sum_{t=0}^{M} \binom{M}{t} \left(\Omega_\ell\right)^t \left(1 - \Omega_\ell\right)^{M-t} \times \prod_{k=1}^{t} \Xi_k, \tag{33}$$

and

$$TP_{TSRS} \triangleq \left(1 - OP_{TSRS}\right) \mathrm{R}_2. \tag{34}$$

where Ω_ℓ and Ξ_k are given in (24) and (30) respectively.

5 POWER ALLOCATION BASED RELAY SELECTION (PA)

The relay can successfully decode the messages x_1 and x_2 if the following condition satisfies

$$\begin{cases} \log_2\left(1 + \frac{\upsilon_1\rho_s|h_k|^2}{\upsilon_2\rho_s|h_k|^2 + \rho_r|f_k|^2 + 1}\right) \geq R_1 \\ \log_2\left(1 + \frac{\upsilon_2\rho_s|h_k|^2}{\rho_r|f_k|^2 + 1}\right) \geq R_2. \end{cases} \tag{35}$$

It is equivalent with $|h_k|^2 \geq \chi$, where $\chi = \max\left(\left(\frac{\delta_1^{\text{th}}}{\upsilon_1 - \upsilon_2 \delta_1^{\text{th}}}, \frac{\delta_2^{\text{th}}}{\upsilon_2}\right)\left(\frac{\rho_r |f_k|^2 + 1}{\rho_s}\right)\right.$.

Recall that D_1 has the priority to be served, i.e., the target rate requirements of D_1 need to be met as follows:

$$\log_2 \quad 1 + \frac{\vartheta_1 \rho_r |g_{k,1}|^2}{\vartheta_2 \rho_r |g_{k,1}|^2 + 1} \geq R_1, \tag{36}$$

The maximal power allocation factor ϑ_2 can be expressed as follows:

$$\log_2 \quad 1 + \frac{\vartheta_1 \rho_r |g_{k,1}|^2}{\vartheta_2 \rho_r |g_{k,1}|^2 + 1} \geq R_1, \tag{37}$$

Then, it can be simplified as

$$\vartheta_2 = \max \quad 0, \frac{\rho_r |g_{k,1}|^2 - \delta_1^{\text{th}}}{\rho_r |g_{k,1}|^2 \left(1 + \delta_1^{\text{th}}\right)} \tag{38}$$

Note that if $|g_{k,1}|^2 > \frac{\delta_1^{\text{th}}}{\rho_r}$, the condition is always possible. That is to say, D_1 can always successfully detect its own message under the condition $|g_{k,1}|^2 > \frac{\delta_1^{\text{th}}}{\rho_r}$.

A set of active relays which can satisfy the QoS requirements of D_1 can be defined as follows:

$$\mathcal{B}_{\mathcal{R}} = \left\{ r_i : r_i \in \mathcal{S}_{\mathcal{R}}, |h_{r_i}|^2 \geq \chi, |g_{r_i,d_1}|^2 > \frac{\delta_1^{\text{th}}}{\rho_r} \right\} \tag{39}$$

The best relay is selected to serve D_2

$$b = \arg \max_{i \in \mathcal{B}_{\mathcal{R}}} \left\{ |g_{r_i,d_2}|^2 \right\} \tag{40}$$

Furthermore, in order to ensure D_2 can be achieve a high data rate, we impose a constraint that the SIC can be successfully carried out at D_2

$$\log_2 \quad 1 + \frac{\vartheta_1 \rho_r |g_{r_b,d_2}|^2}{\vartheta_2 \rho_r |g_{r_b,d_2}|^2 + 1} \geq R_1, \tag{41}$$

It can be simplified to

$$\vartheta_2 = \max \quad 0, \frac{\rho_r |g_{r_b,d_2}|^2 - \delta_1^{\text{th}}}{\rho_r |g_{r_b,d_2}|^2 \left(1 + \delta_1^{\text{th}}\right)} \tag{42}$$

The power allocation factor ϑ_2 can be rewritten as (43)

$$\vartheta_2 = \min \left\{ \frac{\rho_r |g_{r_b,d_1}|^2 - \delta_1^{\text{th}}}{\rho_r |g_{r_b,d_1}|^2 \left(1 + \delta_1^{\text{th}}\right)}, \max \quad 0, \frac{\rho_r |g_{r_b,d_2}|^2 - \delta_1^{\text{th}}}{\rho_r |g_{r_b,d_2}|^2 \left(1 + \delta_1^{\text{th}}\right)} \right\}. \tag{43}$$

The power allocation coefficient ϑ_2 depends on δ_1^{th} and the channel fading gains from the best relay to the two users. Furthermore, note that if $|g_{r_b,d_2}|^2 < \frac{\delta_1^{\text{th}}}{\rho_r}$,

the power allocation factor becomes zero. $\vartheta_2 = 0$, since the relay allocates all the power to serve D_1, when the target rate of the D_1 is high or the channel condition between the best relay and D_2 is poor. The coverage probability of D_2 is calculated as follow

$$\begin{aligned}
\overline{\mathrm{OP}_2^{\mathrm{PA}}} &= \sum_{i=1}^{M} \Pr\left\{\log_2\left(1+\vartheta_2\rho_r|g_{r_b,d_2}|^2\right) \geq R_2, |\mathcal{B}_{\mathcal{R}}| = i\right\}\Bigg(\\
&= \sum_{i=1}^{M} \Pr\left\{1\Bigg(+\vartheta_2\rho_r|g_{r_b,d_2}|^2 \geq 2^{R_2}, |\mathcal{B}_{\mathcal{R}}| = i\right\} \\
&= \sum_{i=1}^{M} \Pr\left\{\vartheta_2\Bigg(\rho_r|g_{r_b,d_2}|^2 \geq 2^{R_2}-1, |\mathcal{B}_{\mathcal{R}}| = i\right\} \\
&= \sum_{i=1}^{M} \underbrace{\Pr\left\{\vartheta_2 \geq \frac{\delta_2^{\mathrm{th}}}{\rho_r|g_{r_b,d_2}|^2} \,|\, |\mathcal{B}_{\mathcal{R}}| = i\right\}}_{\eta_1} \Pr\{|\mathcal{B}_{\mathcal{R}}| = i\}.
\end{aligned} \tag{44}$$

Proposition 3: The outage probability of the consideblack system can be expressed as

$$\begin{aligned}
\mathrm{OP}_2^{\mathrm{PA}} =& 1 - \overline{\mathrm{OP}_2^{\mathrm{PA}}} \\
=& 1 - \sum_{i=1}^{M} \underbrace{\Pr\left\{\vartheta_2 \geq \frac{\delta_2^{\mathrm{th}}}{\rho_r|g_{r_b,d_2}|^2}, |\mathcal{B}_{\mathcal{R}}| = i\right\}}_{\triangleq \eta_1} \Pr\{|\mathcal{B}_{\mathcal{R}}| = i\} \\
=& 1 - \frac{1}{\exp\left(-\frac{\delta_1^{\mathrm{th}}}{\rho_r\beta_{g_{r_k,d_1}}}\right) \sum\limits_{n_3=0}^{m_{g_{r_k,d_1}}-1} \frac{\left(\delta_1^{\mathrm{th}}\right)^{n_3}}{n_3!\rho_r^{n_3}\beta_{g_{r_k,d_1}}^{n_3}}} \Bigg(\\
&\times \Bigg(\Bigg(\exp\left(-\frac{\delta_1^{\mathrm{th}}}{\rho_r\beta_{g_{r_k,d_1}}}\right) \sum_{n=0}^{m_{g_{r_k,d_1}}-1} \frac{1}{n!\beta_{g_{r_k,d_1}}^{n}} \left(\frac{\delta_1^{\mathrm{th}}}{\rho_r}\right)^n \\
&\quad - \exp\left(-\frac{\varepsilon_2\delta_1^{\mathrm{th}}}{\rho_r\beta_{g_{r_k,d_1}}(\varepsilon_2-\varepsilon_1)}\right) \sum_{n=0}^{m_{g_{r_b,d_1}}-1} \frac{1}{n!\beta_{g_{r_b,d_1}}^{n}} \left(\frac{\varepsilon_2\delta_1^{\mathrm{th}}}{\rho_r(\varepsilon_2-\varepsilon_1)}\right)^n \Bigg)^i \\
&\quad \times \left(1 - \exp\left(-\frac{1}{\beta_{g_{r_k,d_2}}}\frac{\varepsilon_2}{\rho_r}\right) \sum_{n_1=0}^{m_{g_{r_k,d_2}}-1} \frac{1}{n_1!\beta_{g_{r_k,d_2}}^{n_1}} \left(\frac{\varepsilon_2}{\rho_r}\right)^{n_1}\right)^i \Bigg) \\
&- \frac{1}{\Gamma\left(m_{g_{r_k,d_1}}\right)\beta_{g_{r_k,d_1}}^{m_{g_{r_k,d_1}}}} \int_{\frac{\varepsilon_2}{\rho_r}}^{\infty} \frac{\varepsilon_1\delta_1^{\mathrm{th}}}{(\rho_r y-\varepsilon_1)^2} \left(1 - \exp\left(-\left(\frac{y}{\beta_{g_{r_k,d_2}}}\right)^{m_{g_{r_k,d_2}}-1} \sum_{n_2=0} \frac{1}{n_2!\beta_{g_{r_k,d_2}}^{n_2}} y^{n_2}\right)^i\right) \\
&\quad \times \left(\frac{\delta_1^{\mathrm{th}} y}{\rho_r y-\varepsilon_1}\right)^{m_{g_{r_k,d_1}}-1} \exp\left(-\frac{\delta_1^{\mathrm{th}} y}{\beta_{g_{r_k,d_1}}(\rho_r y-\varepsilon_1)}\right)\Bigg) dy
\end{aligned} \tag{45}$$

Table 2 MAIN PARAMETERS IN THE RELATED SIMULATIONS.

–	R_1, R_2	ϑ_1/υ_1	m	M	ρ
Figure 2	$R_1 = 0.5, R_2 = 1$	$\vartheta_1 = \upsilon_1 = 0.7$	$m = 2$	$M = 2/3/4/5/6$	–
Figure 3	$R_1 = 0.5, R_2 = 1$	$\vartheta_1 = \upsilon_1 = 0.7$	$m = 2/3/4/5/6$	$M = 3$	–
Figure 4	$R_1 = 0.1, R_2 = 0.5/$ $R_1 = 0.5, R_2 = 1.0/$ $R_1 = 1.0, R_2 = 1.5/$ $R_1 = 1.5, R_2 = 2.0/$	$\vartheta_1 = \upsilon_1 = 0.7$	$m = 2$	$M = 3$	$--$
Figure 5	$R_1 = 0.5, --$	$\vartheta_1 = \upsilon_1 = 0.6$	$m = 2$	$M = 2/3/4/5/6$	$\rho = 10dB$
Figure 6	$R_1 = 1.0, R_2 = 2.0$	$\vartheta_1 = \upsilon_1 = 0.9$	$m = 2$	$M = 2/3/4/5/6$	$\rho = 10dB$
Figure 7	$R_1 = 1, R_2 = 2.0$	$\vartheta_1 = \upsilon_1 = 0.9$	$m = 1$	M = 2/3/4/5	–
Figure 8	$R_1 = 1.0, R_2 = 2.0$	$\vartheta_1 = \upsilon_1 = 0.7$	$m = 1$	$M = 2/3/4/5$	–
Figure 9	$R_1 = 0.5, R_2 = 2.0$	$\vartheta_1 = \upsilon_1 = 0.75$	$m = 3$	$M = 2/4$	–

Proof: See in appendix C.
The throughput analysis of the consideblack system can be written as

$$TP_2^{PA} \triangleq \left(1 - \mathrm{OP}_2^{\mathrm{PA}}\right) \mathrm{R}_2. \tag{46}$$

6 Numerical Results

Simulations are accomplished for system performance evaluation in MATLAB to obtain role of parameters which have an intuitive effect on FD NOMA networks in term of analytical and simulation results. We set main parameters as in Table 2. In this section, the analytical results together with Monte Carlo simulations in terms of outage probability and throughput are presented to prove that the advantage of FD-NOMA compablack with the counterpart.

In Fig. 2, we demonstrate the outage probability in TSRS scheme against the increasing values of transmit SNR at the BS. In particular, by increasing the number of intermediate relay, there are performance gap of outage probability among three consideblack cases $M = 2, 3, ..., 6$. As the most interesting point, equal performance gap for cases of M as varying ρ from 25 to 40. It is worth noting that the outage significantly blackuces by increasing ρ from 5 to 25. It is very valuable result as tight matching between Monte-Carlo and analytical analysis based simulations.

Next, the impacts of different values m of the Nakagami-m channels on outage performance of the consideblack system can be seen in Fig. 3. It can be seen clearly from the figure that with the higher value of m exhibits a better outage behavior in whole range of ρ. This is because larger m means the corresponding channel could be better. The Fig. 3 also depicts that the outage probability of the users can be blackuced by increasing m parameter.

In Fig. 4, we can see trends of outage performance versus transmit SNR at the BS ρ. At higher requirement of target rates R_1, R_2, outage performance of

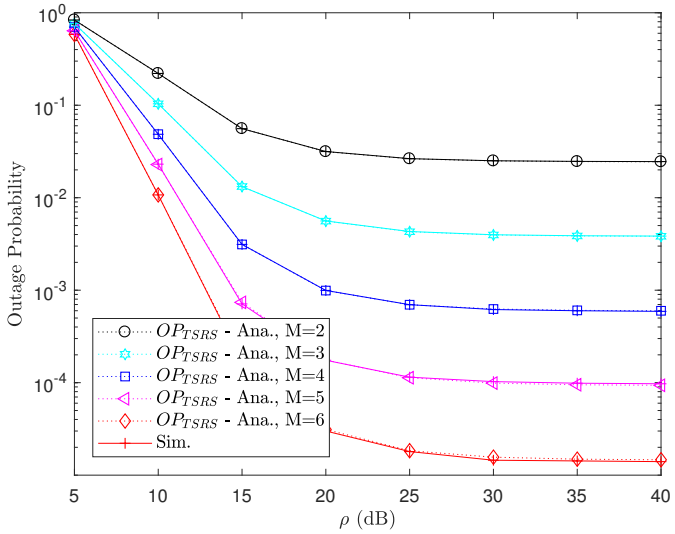

Fig. 2 TSRS: Effect of M on the outage performance for cooperative NOMA

.

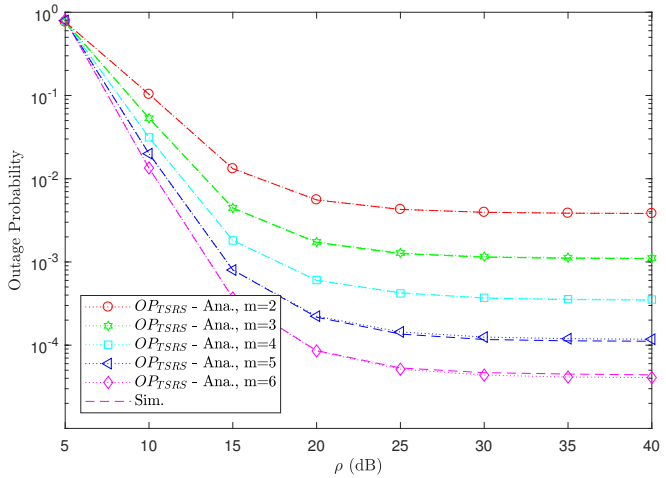

Fig. 3 TSRS: Outage probability versus transmit SNR with different m.

the consideblack system becomes worse. It can be explained that the probability of SINR is computed based on target rate. Therefore, target rates limit performance in term of outage probability.

In Fig. 5, it is obvious to recognize that self-interference at relay leads to change in outage performance of our system. In particular, we can see trends of outage performance be worse at high value of λ_f. When we change values

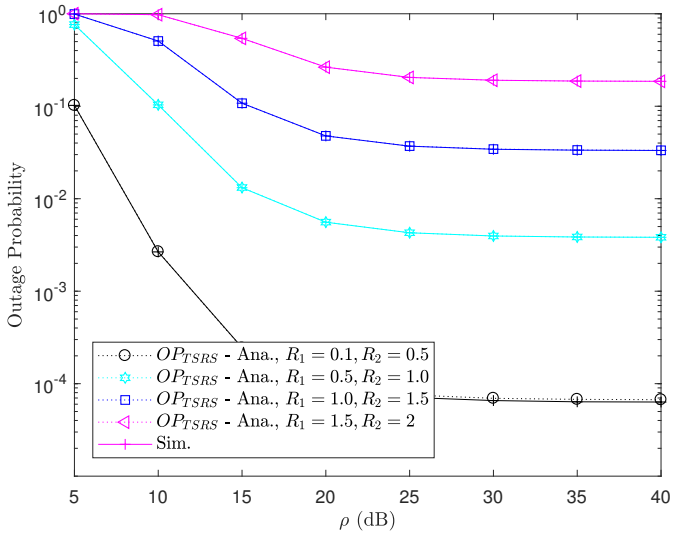

Fig. 4 Effect of users' target rates on cooperative two-stage DF relaying NOMA.

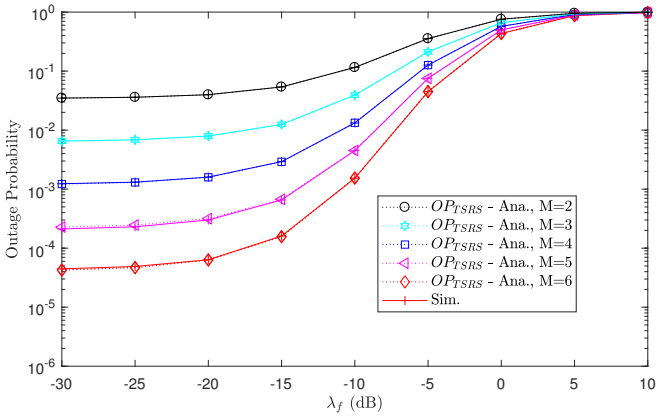

Fig. 5 TSRS: Outage probability versus λ_f.

of M, the outage performance gaps are clearer at low range of λ_f. Therefore, by blackucing self-interference, the outage performance can be remained at acceptable value. In Fig. 6, the limitation of requiblack target rate R_2 can be verified by varying it from 1 to 5. We can conclude that the consideblack system would be stop its operation if we require very high value of target rate. This can be explained that target rate exists in the expression to compute outage probability. Other impacts of parameters on such outage probability can be seen similarly as Fig. 4.

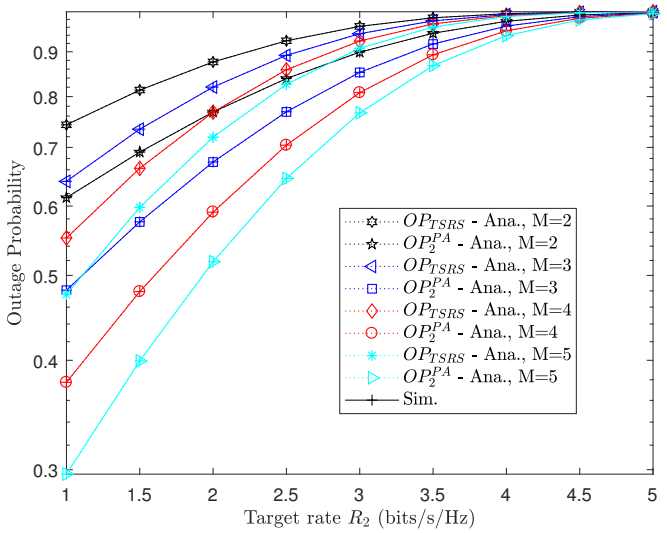

Fig. 6 Outage probability versus R_2.

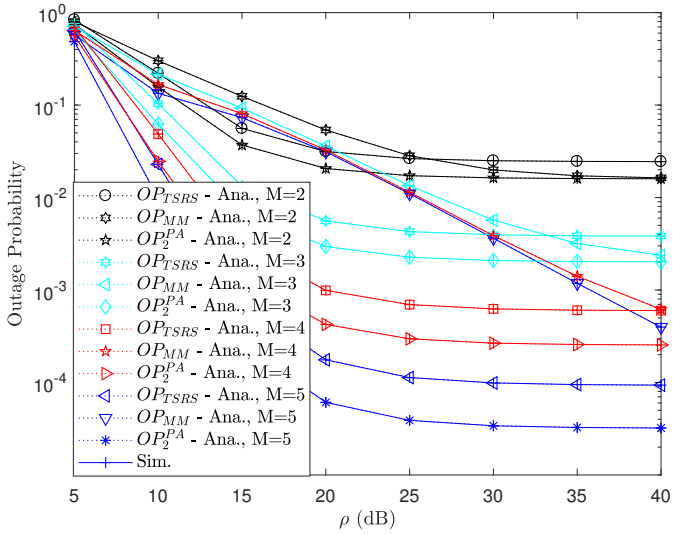

Fig. 7 Outage comparison among three schemes TSRS, MM and PA.

Fig. 7 provides us the comparison between NOMA systems relying on TSRS, MM and PA schemes. It can be concluded that system relying on PA scheme is the best among consideblack schemes regardless the impacts M and SNR ρ. However, performance of two methods, namely MM and PA, would be the same once such SNR is greater than 40. The main reason is that outage

probability does not rely on any parameters at high SNR region. This result give us important recommendation to decide which relay selection is suitable with specific demand of systems.

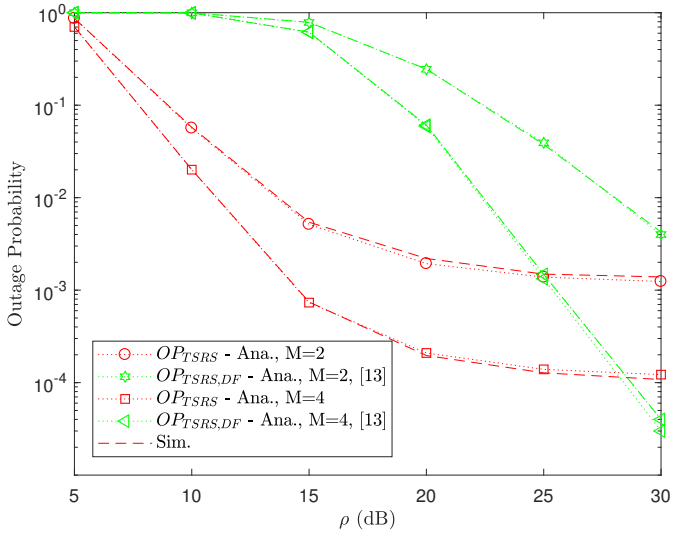

Fig. 8 The comparison between TSRS and work in [13] reference.

Although outage performance can be controlled by M and target rate, outage performance comparison is presented in Fig. 8. The system relying on TSRS exhibits its performance gap in these compablack cases, i.e. $M = 2$, $M = 4$. It can be seen intuitively that our schemes outperform that in [13]. However, at high SNR region, the scheme reported in [13] can improve performance significantly, while our schemes show the floor outage performance at the point ρ greater than 30 dB.

Although outage performance can be controlled by M and target rates, performance gaps of throughput in Fig. 9 are small. When ρ goes to 35 dB, such throughput is approximate 2 (bps/Hz). Similarly, the throughput is limited at high SNR region. The reason is that throughput depends on the fixed target rate and outage probability, but outage probability can not improve at high SNR region.

7 Conclusions

A framework of NOMA system for downlink is studied under various scenarios of RS schemes. We can achieve improvement in specific RS scheme. We derived closed-form expressions to show performance of system in terms of outage behavior and throughput. Such improvement can be evaluated for two

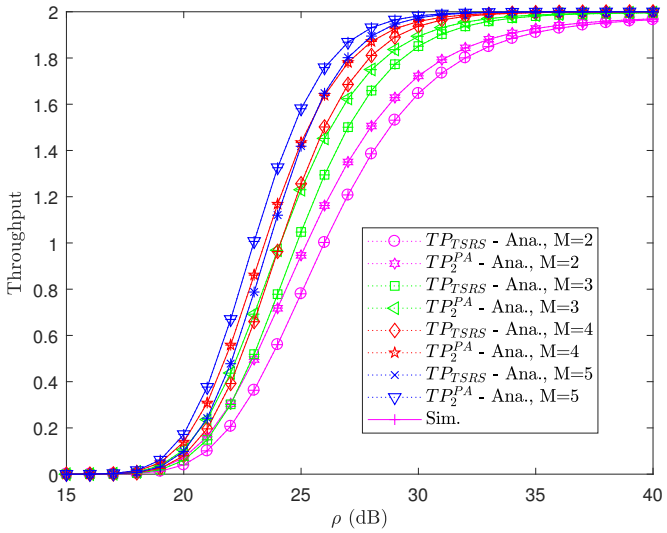

Fig. 9 The throughput performance

metrics such as outage probability and throughput. Further studies are expected to exploit the potential of the NOMA system serving multiple users with performance improvement controlled by main parameters such as the power allocation factors, the number of relay, and target rates.

Appendix A: Proof of Lemma 1

It is straight forward to obtain Lemma 1 as below

$$\begin{aligned}\Phi(a,b,k) &= \Pr\left(a|h_k|^2 \geq b|f_k|^2+1\right)\\ &= \int_0^\infty \left(1-F_{|h_k|^2}\left(\frac{bx+1}{a}\right)\right) f_{|f_k|^2}(x)\,dx\\ &= \frac{\exp\left(-1/(a\beta_h)\right)}{\Gamma(m_f)\,\beta_f^{m_f}} \sum_{n=0}^{m_h-1} \frac{1}{\beta_h^n a^n} \int_0^\infty \frac{(bx+1)^n x^{m_f-1}}{n!} \mathrm{e}^{-x\left(\frac{1}{\beta_f}+\frac{b}{a\beta_h}\right)} dx.\end{aligned} \tag{47}$$

It can be simplified $\Phi(a,b,k)$ as below

$$\begin{aligned}\Phi(a,b,k) =& \frac{\exp(-1/(a\beta_h))}{\Gamma(m_f)\,\beta_f^{m_f}} \sum_{n=0}^{m_h-1}\sum_{k=0}^{n}\binom{n}{k}\frac{1}{\beta_h^n a^n}\frac{b^k}{n!}\int_0^\infty x^{k+m_f-1}\mathrm{e}^{-x\left(\frac{1}{\beta_f}+\frac{b}{a\beta_h}\right)}dx \\ =& \frac{\exp(-1/(a\beta_h))}{\Gamma(m_f)\,\beta_f^{m_f}} \sum_{n=0}^{m_h-1}\sum_{k=0}^{n}\binom{n}{k}\frac{1}{\beta_h^n a^n}\frac{b^k}{n!}\left(\frac{1}{\beta_f}+\frac{b}{a\beta_h}\right)^{-k-m_f}\Gamma(k+m_f).\end{aligned} \tag{48}$$

The last step can be obtained by applying (Eq. 1.111) in [39], and the integration is derived thank to (Eq. 3.381.4) in [39]. Thus, the lemma is proved.

Appendix B: Proof of Proposition 1

Based on the definition of MM mode using (18), the system outage is given by (49), shown in the top of the next page.

$$\begin{aligned}OP_{MM} =& \Pr\left(\min\left(\frac{\gamma_{r_{b_{MM}}\leftarrow 1}}{\delta_1^{\mathrm{th}}},\frac{\gamma_{r_{b_{MM}},d_1}}{\delta_1^{\mathrm{th}}},\frac{\gamma_{r_{b_{MM}},d_2\leftarrow 1}}{\delta_1^{\mathrm{th}}},\frac{\gamma_{r_{b_{MM}}\leftarrow 2}}{\delta_2^{\mathrm{th}}},\frac{\gamma_{r_{b_{MM}},d_2}}{\delta_2^{\mathrm{th}}}\right)<1\right) \\ =& \Pr\left(\max_{k\in\mathcal{S}_{\mathcal{R}}}\left(\min\left(\frac{\gamma_{r_k\leftarrow 1}}{\delta_1^{\mathrm{th}}},\frac{\gamma_{r_k,d_1}}{\delta_1^{\mathrm{th}}},\frac{\gamma_{r_k,d_2\leftarrow 1}}{\delta_1^{\mathrm{th}}},\frac{\gamma_{r_k\leftarrow 2}}{\delta_2^{\mathrm{th}}},\frac{\gamma_{r_k,d_2}}{\delta_2^{\mathrm{th}}}\right)\right)<1\right)\end{aligned} \tag{49}$$

Additionally, due to the independence of channels, (49) can be simplified as

$$\begin{aligned}OP_{MM} =& \prod_{k=1}^{M}\Pr\left(\min\left(\frac{\gamma_{r_k\leftarrow 1}}{\delta_1^{\mathrm{th}}},\frac{\gamma_{r_k,d_1}}{\delta_1^{\mathrm{th}}},\frac{\gamma_{r_k,d_2\leftarrow 1}}{\delta_1^{\mathrm{th}}},\frac{\gamma_{r_k\leftarrow 2}}{\delta_2^{\mathrm{th}}},\frac{\gamma_{r_k,d_2}}{\delta_2^{\mathrm{th}}}\right)<1\right) \\ =& \prod_{k=1}^{M}1-\Pr\left(\min\left(\frac{\gamma_{r_k\leftarrow 1}}{\delta_1^{\mathrm{th}}},\frac{\gamma_{r_k,d_1}}{\delta_1^{\mathrm{th}}},\frac{\gamma_{r_k,d_2\leftarrow 1}}{\delta_1^{\mathrm{th}}},\frac{\gamma_{r_k\leftarrow 2}}{\delta_2^{\mathrm{th}}},\frac{\gamma_{r_k,d_2}}{\delta_2^{\mathrm{th}}}\right)\geq 1\right) \\ =& \prod_{k=1}^{M}1-\Pr\left(\frac{\gamma_{r_k\leftarrow 1}}{\delta_1^{\mathrm{th}}}\geq 1,\frac{\gamma_{r_k,d_1}}{\delta_1^{\mathrm{th}}}\geq 1,\frac{\gamma_{r_k,d_2\leftarrow 1}}{\delta_1^{\mathrm{th}}}\geq 1,\frac{\gamma_{r_k\leftarrow 2}}{\delta_2^{\mathrm{th}}}\geq 1,\frac{\gamma_{r_k,d_2}}{\delta_2^{\mathrm{th}}}\geq 1\right).\end{aligned} \tag{50}$$

The expression in multiplication can be further expressed as (51).

$$\Pr\left(\min\left(\frac{\gamma_{r_k\leftarrow 1}}{\delta_1^{\mathrm{th}}},\frac{\gamma_{r_k\leftarrow 2}}{\delta_2^{\mathrm{th}}}\right)\geq 1\right)\Pr\left(\frac{\gamma_{r_k,d_1}}{\delta_1^{\mathrm{th}}}\geq 1\right)\Pr\left(\min\left(\frac{\gamma_{r_k,d_2\leftarrow 1}}{\delta_1^{\mathrm{th}}},\frac{\gamma_{r_k,d_2}}{\delta_2^{\mathrm{th}}}\right)\geq 1\right) \tag{51}$$

Finally, with the same step in (45), the Theorem 1 is derived.

This completes the proof.

Appendix C: Proof of Proposition 3

The above probability η_1 can be calculated as

$$\begin{aligned}
\eta_1 =& \Pr\left\{\min\left\{\left(\frac{\rho_r|g_{r_b,d_1}|^2-\delta_1^{\text{th}}}{\rho_r|g_{r_b,d_1}|^2\left(1+\delta_1^{\text{th}}\right)}, \max\quad 0, \frac{\rho_r|g_{r_b,d_2}|^2-\delta_1^{\text{th}}}{\rho_r|g_{r_b,d_2}|^2\left(1+\delta_1^{\text{th}}\right)}\right)\right\} \geq \frac{\delta_2^{\text{th}}}{\rho_r|g_{r_b,d_2}|^2} : r_b \in \mathcal{B}_{\mathcal{R}}\right\} \\
=& \Pr\left\{|g_{r_b,d_2}|^2 > \frac{\delta_1^{\text{th}}}{\rho_r}, \min\left\{\left(\frac{\rho_r|g_{r_b,d_1}|^2-\delta_1^{\text{th}}}{\rho_r|g_{r_b,d_1}|^2\left(1+\delta_1^{\text{th}}\right)}, \frac{\rho_r|g_{r_b,d_2}|^2-\delta_1^{\text{th}}}{\rho_r|g_{r_b,d_2}|^2\left(1+\delta_1^{\text{th}}\right)}\right\} \geq \frac{\delta_2^{\text{th}}}{\rho_r|g_{r_b,d_2}|^2} : r_b \in \mathcal{B}_{\mathcal{R}}\right\}\right. \\
&+ \underbrace{\Pr\left\{|g_{r_b,d_2}|^2 \leq \frac{\delta_1^{\text{th}}}{\rho_r}, 0 \geq \frac{\delta_2^{\text{th}}}{\rho_r|g_{r_b,d_2}|^2} : r_b \in \mathcal{B}_{\mathcal{R}}\right\}}_{=0} \\
=& \Pr\left\{|g_{r_b,d_2}|^2 > \frac{\delta_1^{\text{th}}}{\rho_r}, \underbrace{\frac{\rho_r|g_{r_b,d_1}|^2-\delta_1^{\text{th}}}{\rho_r|g_{r_b,d_1}|^2\left(1+\delta_1^{\text{th}}\right)} \geq \frac{\delta_2^{\text{th}}}{\rho_r|g_{r_b,d_2}|^2}}_{\triangleq\varpi_1}, \underbrace{\frac{\rho_r|g_{r_b,d_2}|^2-\delta_1^{\text{th}}}{\rho_r|g_{r_b,d_2}|^2\left(1+\delta_1^{\text{th}}\right)} \geq \frac{\delta_2^{\text{th}}}{\rho_r|g_{r_b,d_2}|^2}}_{\triangleq\varpi_2} : r_b \in \mathcal{B}_{\mathcal{R}}\right\}
\end{aligned} \tag{52}$$

With the condition $\rho_r|g_{r_b,d_2}|^2-\delta_1^{\text{th}} > 0 \Leftrightarrow |g_{r_b,d_2}|^2 > \frac{\delta_1^{\text{th}}}{\rho_r} \Rightarrow \max\left(0, \frac{\rho_r|g_{r_b,d_2}|^2-\delta_1^{\text{th}}}{\rho_r|g_{r_b,d_2}|^2\left(1+\delta_1^{\text{th}}\right)}\right) = \frac{\rho_r|g_{r_b,d_2}|^2-\delta_1^{\text{th}}}{\rho_r|g_{r_b,d_2}|^2\left(1+\delta_1^{\text{th}}\right)}$.
We calculate ϖ_1

$$\begin{aligned}
\varpi_1 =& \frac{\rho_r|g_{r_b,d_1}|^2-\delta_1^{\text{th}}}{\rho_r|g_{r_b,d_1}|^2\left(1+\delta_1^{\text{th}}\right)} \geq \frac{\delta_2^{\text{th}}}{\rho_r|g_{r_b,d_2}|^2} \\
=& |g_{r_b,d_1}|^2 \geq \frac{\delta_1^{\text{th}}|g_{r_b,d_2}|^2}{\rho_r|g_{r_b,d_2}|^2-\delta_2^{\text{th}}\left(1+\delta_1^{\text{th}}\right)} \\
=& |g_{r_b,d_1}|^2 \geq \frac{\delta_1^{\text{th}}|g_{r_b,d_2}|^2}{\rho_r|g_{r_b,d_2}|^2-\varepsilon_1},
\end{aligned} \tag{53}$$

where $\rho_r|g_{r_b,d_1}|^2-\delta_1^{\text{th}} > 0 \Leftrightarrow |g_{r_b,d_1}|^2 > \frac{\delta_1^{\text{th}}}{\rho_r}$ and $\varepsilon_1 = \delta_2^{\text{th}}\left(1+\delta_1^{\text{th}}\right)$.
We calculate ϖ_2

$$\begin{aligned}
\varpi_2 =& \frac{\rho_r|g_{r_b,d_2}|^2-\delta_1^{\text{th}}}{\rho_r|g_{r_b,d_2}|^2\left(1+\delta_1^{\text{th}}\right)} \geq \frac{\delta_2^{\text{th}}}{\rho_r|g_{r_b,d_2}|^2} \\
=& |g_{r_b,d_2}|^2 \geq \frac{\delta_2^{\text{th}}\left(1+\delta_1^{\text{th}}\right)+\delta_1^{\text{th}}}{\rho_r} \\
=& |g_{r_b,d_2}|^2 \geq \frac{\varepsilon_2}{\rho_r},
\end{aligned} \tag{54}$$

where $\begin{cases} |g_{r_b,d_2}|^2 > \frac{\delta_1^{\text{th}}}{\rho_r} \\ |g_{r_b,d_2}|^2 \geq \frac{\varepsilon_2}{\rho_r} \end{cases} \Leftrightarrow |g_{r_b,d_2}|^2 > \max\left(\frac{\delta_1^{\text{th}}}{\rho_r}, \frac{\varepsilon_2}{\rho_r}\right) \Rightarrow |g_{r_b,d_2}|^2 \geq \frac{\varepsilon_2}{\rho_r}$ and $\varepsilon_2 = \varepsilon_1 + \delta_1^{\text{th}}$.
From ϖ_1 and ϖ_2, we have new result as follow

$$\eta_1 = \Pr\left\{|g_{r_b,d_1}|^2 \geq \frac{\delta_1^{\text{th}}|g_{r_b,d_2}|^2}{\rho_r|g_{r_b,d_2}|^2 - \varepsilon_1}, |g_{r_b,d_2}|^2 \geq \frac{\varepsilon_2}{\rho_r} : |g_{r_b,d_1}|^2 > \frac{\delta_1^{\text{th}}}{\rho_r}\right\}. \quad (55)$$

We apply the Bayes theorem: $\mathrm{P}(\mathrm{A}'|\mathrm{C}) = \frac{\mathrm{P}(\mathrm{A}',\mathrm{C})}{\mathrm{P}(\mathrm{C})}$, where $\mathrm{P}(\mathrm{A}',\mathrm{C})$ is computed as follow, while $\mathrm{P}(\mathrm{C}) = \left\{|g_{r_b,d_1}|^2 > \frac{\delta_1^{\text{th}}}{\rho_r}\right\}$.

$$\mathrm{P}(\mathrm{A}',\mathrm{C}) = \left\{|g_{r_b,d_1}|^2 \geq \frac{\delta_1^{\text{th}}|g_{r_b,d_2}|^2}{\rho_r|g_{r_b,d_2}|^2 - \varepsilon_1}, |g_{r_b,d_2}|^2 \geq \frac{\varepsilon_2}{\rho_r}, |g_{r_b,d_1}|^2 > \frac{\delta_1^{\text{th}}}{\rho_r}\right\}. \quad (56)$$

It is worth noting that $|g_{r_b,d_1}|^2 \geq \frac{\delta_1^{\text{th}}}{\rho_r - \frac{\varepsilon_1}{|g_{r_b,d_2}|^2}}$ because $\frac{\varepsilon_1}{|g_{r_b,d_2}|^2} \geq 0$.

$$\begin{aligned} &\Rightarrow \rho_r - \frac{\varepsilon_1}{|g_{r_b,d_2}|^2} \leq \rho_r \Leftrightarrow \frac{\delta_1^{\text{th}}|g_{r_b,d_2}|^2}{\rho_r|g_{r_b,d_2}|^2 - \varepsilon_1} > \frac{\delta_1^{\text{th}}}{\rho_r} \\ &\Rightarrow \max\left(\frac{\delta_1^{\text{th}}|g_{r_b,d_2}|^2}{\rho_r|g_{r_b,d_2}|^2 - \varepsilon_1}, \frac{\delta_1^{\text{th}}}{\rho_r}\right) = \frac{\delta_1^{\text{th}}|g_{r_b,d_2}|^2}{\rho_r|g_{r_b,d_2}|^2 - \varepsilon_1}. \end{aligned} \quad (57)$$

After the analysis, η_1 is calculated by

$$\begin{aligned} \eta_1 &= \frac{\mathrm{P}(\mathrm{A}',\mathrm{C})}{\mathrm{P}(\mathrm{C})} \\ &= \frac{\Pr\left\{|g_{r_b,d_1}|^2 \geq \frac{\delta_1^{\text{th}}|g_{r_b,d_2}|^2}{\rho_r|g_{r_b,d_2}|^2 - \varepsilon_1}, |g_{r_b,d_2}|^2 \geq \frac{\varepsilon_2}{\rho_r}, |g_{r_b,d_1}|^2 > \frac{\delta_1^{\text{th}}}{\rho_r}\right\}}{\Pr\left\{|g_{r_b,d_1}|^2 > \frac{\delta_1^{\text{th}}}{\rho_r}\right\}} \\ &= \frac{\Pr\left\{|g_{r_b,d_1}|^2 \geq \max\left\{\frac{\delta_1^{\text{th}}|g_{r_b,d_2}|^2}{\rho_r|g_{r_b,d_2}|^2 - \varepsilon_1}, \frac{\delta_1^{\text{th}}}{\rho_r}\right\}, |g_{r_b,d_2}|^2 \geq \frac{\varepsilon_2}{\rho_r}\right\}}{\Pr\left\{|g_{r_b,d_1}|^2 > \frac{\delta_1^{\text{th}}}{\rho_r}\right\}} \\ &= \frac{\Pr\left\{|g_{r_b,d_1}|^2 \geq \frac{\delta_1^{\text{th}}|g_{r_b,d_2}|^2}{\rho_r|g_{r_b,d_2}|^2 - \varepsilon_1}, |g_{r_b,d_2}|^2 \geq \frac{\varepsilon_2}{\rho_r}\right\}}{\Pr\left\{|g_{r_b,d_1}|^2 > \frac{\delta_1^{\text{th}}}{\rho_r}\right\}}. \end{aligned} \quad (58)$$

We have

$$\eta_1 = \frac{\Pr\left\{|g_{r_b,d_1}|^2 \geq \frac{\delta_1^{\text{th}}|g_{r_b,d_2}|^2}{\rho_r|g_{r_b,d_2}|^2-\varepsilon_1}, |g_{r_b,d_2}|^2 \geq \frac{\varepsilon_2}{\rho_r}\right\}}{1-F_{|g_{r_b,d_1}|^2}\left(\frac{\delta_1^{\text{th}}}{\rho_r}\right)}. \tag{59}$$

Now, we have new variables as $X = |g_{r_b,d_1}|^2, Y = |g_{r_b,d_2}|^2$. Next, η_1 is calculated as follow

$$\begin{aligned}\eta_1 =& \frac{\int_{\frac{\varepsilon_2}{\rho_r}}^{\infty}\left(1-F_X\left(\frac{\delta_1^{\text{th}}Y}{\rho_r Y-\varepsilon_1}\right)\right)f_Y(y)\,dy}{1-F_{|g_{r_b,d_1}|^2}\left(\frac{\delta_1^{\text{th}}}{\rho_r}\right)} \\ =& \frac{\Phi_1}{\Phi_2}\end{aligned} \tag{60}$$

It is necessary to calculate Φ_1 and Φ_2 respectively as bellows. By using partial integration, we have

$$\begin{aligned}\Phi_1 =& \int_{\frac{\varepsilon_2}{\rho_r}}^{\infty}\left(1-F_X\left(\frac{\delta_1^{\text{th}}Y}{\rho_r Y-\varepsilon_1}\right)\right)f_Y(y)\,dy \\ =& \int_{\frac{\varepsilon_2}{\rho_r}}^{\infty}\left(1-F_{|g_{r_k,d_1}|^2}\left(\frac{\delta_1^{\text{th}}y}{\rho_r y-\varepsilon_1}\right)\right)f_{|g_{r_k,d_2}|^2}(y)\,dy.\end{aligned} \tag{61}$$

Then, Φ_1 is rewritten as

$$\begin{aligned}\Phi_1 =& \underbrace{\left(1-F_{|g_{r_k,d_1}|^2}\left(\frac{\delta_1^{\text{th}}y}{\rho_r y-\varepsilon_1}\right)\right)F_{|g_{r_k,d_2}|^2}(y)}_{\triangleq\varphi_1} \\ &- \underbrace{\int_{\frac{\varepsilon_2}{\rho_r}}^{\infty}\frac{\varepsilon_1\delta_1^{\text{th}}}{(\rho_r y-\varepsilon_1)^2}F_{|g_{r_k,d_2}|^2}(y)\,f_{|g_{r_k,d_1}|^2}\left(\frac{\delta_1^{\text{th}}y}{\rho_r y-\varepsilon_1}\right)dy}_{\triangleq\varphi_2},\end{aligned} \tag{62}$$

where φ_1 and φ_2 are computed as follows

$$\begin{aligned}
\varphi_1 &= \left(1 - F_{|g_{r_k,d_1}|^2}\left(\frac{\delta_1^{\text{th}} y}{\rho_r y - \varepsilon_1}\right)\right) F_{|g_{r_k,d_2}|^2}(y) \Big|_{\frac{\varepsilon_2}{\rho_r}}^{\infty} \\
&= \left(1 - F_{|g_{r_k,d_1}|^2}\left(\frac{\delta_1^{\text{th}}}{\rho_r}\right)\right) - \left(1 - F_{|g_{r_k,d_1}|^2}\left(\frac{\varepsilon_2 \delta_1^{\text{th}}}{\rho_r(\varepsilon_2 - \varepsilon_1)}\right)\right) \\
&\quad \times \left(1 - \mathrm{e}^{-\frac{\varepsilon_2}{\beta_{g_{r_k,d_2}} \rho_r}} \sum_{n_1=0}^{m_{g_{r_k,d_2}}-1} \frac{1}{n_1! \beta_{g_{r_k,d_2}}^{n_1}} \left(\frac{\varepsilon_2}{\rho_r}\right)^{n_1}\right)^i \\
&= \mathrm{e}^{-\frac{\delta_1^{\text{th}}}{\rho_r \beta_{g_{r_k,d_1}}}} \sum_{n=0}^{m_{g_{r_k,d_1}}-1} \frac{1}{n! \beta_{g_{r_k,d_1}}^{n}} \left(\frac{\delta_1^{\text{th}}}{\rho_r}\right)^{n} \\
&\quad - \mathrm{e}^{-\frac{\varepsilon_2 \delta_1^{\text{th}}}{\rho_r \beta_{g_{r_k,d_1}} (\varepsilon_2 - \varepsilon_1)}} \sum_{n=0}^{m_{g_{r_b,d_1}}-1} \frac{1}{n! \beta_{g_{r_b,d_1}}^{n}} \left(\frac{\varepsilon_2 \delta_1^{\text{th}}}{\rho_r(\varepsilon_2 - \varepsilon_1)}\right)^{n} \\
&\quad \times \left(1 - \mathrm{e}^{-\frac{\varepsilon_2}{\beta_{g_{r_k,d_2}} \rho_r}} \sum_{n_1=0}^{m_{g_{r_k,d_2}}-1} \frac{1}{n_1! \beta_{g_{r_k,d_2}}^{n_1}} \left(\frac{\varepsilon_2}{\rho_r}\right)^{n_1}\right)^i.
\end{aligned} \tag{63}$$

$$\begin{aligned}
\varphi_2 &= \int_{\frac{\varepsilon_2}{\rho_r}}^{\infty} \frac{\varepsilon_1 \delta_1^{\text{th}}}{(\rho_r y - \varepsilon_1)^2} F_{|g_{r_k,d_2}|^2}(y) f_{|g_{r_k,d_1}|^2}\left(\frac{\delta_1^{\text{th}} y}{\rho_r y - \varepsilon_1}\right) dy \\
&= \frac{1}{\Gamma\left(m_{g_{r_k,d_1}}\right) \beta_{g_{r_k,d_1}}^{m_{g_{r_k,d_1}}}} \int_{\frac{\varepsilon_2}{\rho_r}}^{\infty} \frac{\varepsilon_1 \delta_1^{\text{th}}}{(\rho_r y - \varepsilon_1)^2} \left(1 - \mathrm{e}^{-\frac{y}{\beta_{g_{r_k,d_2}}}} \sum_{n_2=0}^{m_{g_{r_k,d_2}}-1} \frac{1}{n_2! \beta_{g_{r_k,d_2}}^{n_2}} y^{n_2}\right)^i \\
&\quad \times \left(\frac{\delta_1^{\text{th}} y}{\rho_r y - \varepsilon_1}\right)^{m_{g_{r_k,d_1}}-1} \mathrm{e}^{-\frac{\delta_1^{\text{th}} y}{\beta_{g_{r_k,d_1}}(\rho_r y - \varepsilon_1)}} dy.
\end{aligned} \tag{64}$$

Since the CDF of $|g_{r_b,d_2}|^2$, e.g. , $F_Y(y) = \left(F_{|g_{r_b,d_2}|^2}(y)\right)^i$, then it can be

achieved PDF as follow

$$\begin{aligned} f_{|g_{r_k,d_2}|^2}(y) =& \left(\left(F_{|g_{r_b,d_2}|^2}(y) \right)^i \right)' \\ =& i \times \left(F_{|g_{r_b,d_2}|^2}(y) \right)^{i-1} \left(F_{|g_{r_b,d_2}|^2}(y) \right)' \\ =& i \times \left(F_{|g_{r_b,d_2}|^2}(y) \right)^{i-1} f_{|g_{r_b,d_2}|^2}(y) \\ =& i \left(1 - \mathrm{e}^{-\frac{y}{\beta_{g_{r_k,d_2}}}} \sum_{n=0}^{m_{g_{r_k,d_2}}-1} \left(\frac{1}{n! \beta^n_{g_{r_k,d_2}}} y^n \right) \right)^{i-1} \frac{y^{m_{g_{r_b,d_2}}-1}}{\Gamma\left(m_{g_{r_b,d_2}}\right) \beta^{m_{g_{r_b,d_2}}}_{g_{r_b,d_2}}} \mathrm{e}^{-\frac{y}{\beta_{g_{r_b,d_2}}}}. \end{aligned} \tag{65}$$

Finally, we have

$$\begin{aligned} \Phi_1 =& \varphi_1 - \varphi_2 \\ =& \exp\left(-\frac{\delta_1^{\mathrm{th}}}{\rho_r \beta_{g_{r_k,d_1}}} \right) \sum_{n=0}^{m_{g_{r_k,d_1}}-1} \left(\frac{1}{n! \beta^n_{g_{r_k,d_1}}} \left(\frac{\delta_1^{\mathrm{th}}}{\rho_r} \right)^n \right. \\ & - \exp\left(-\frac{\varepsilon_2 \delta_1^{\mathrm{th}}}{\rho_r \beta_{g_{r_k,d_1}} (\varepsilon_2 - \varepsilon_1)} \right) \sum_{n=0}^{m_{g_{r_b,d_1}}-1} \left(\frac{1}{n! \beta^n_{g_{r_b,d_1}}} \left(\frac{\varepsilon_2 \delta_1^{\mathrm{th}}}{\rho_r (\varepsilon_2 - \varepsilon_1)} \right)^n \right. \\ & \times \left(1 - \exp\left(-\frac{1}{\beta_{g_{r_k,d_2}}} \frac{\varepsilon_2}{\rho_r} \right) \sum_{n_1=0}^{m_{g_{r_k,d_2}}-1} \left(\frac{1}{n_1! \beta^{n_1}_{g_{r_k,d_2}}} \left(\frac{\varepsilon_2}{\rho_r} \right)^{n_1} \right) \right)^i \Bigg(\\ & - \frac{1}{\Gamma\left(m_{g_{r_k,d_1}}\right) \beta^{m_{g_{r_k,d_1}}}_{g_{r_k,d_1}}} \int_{\frac{\varepsilon_2}{\rho_r}}^{\infty} \left(\frac{\varepsilon_1 \delta_1^{\mathrm{th}}}{(\rho_r y - \varepsilon_1)^2} \left(1 - \mathrm{e}^{-\frac{y}{\beta_{g_{r_k,d_2}}}} \sum_{n_2=0}^{m_{g_{r_k,d_2}}-1} \frac{1}{n_2! \beta^{n_2}_{g_{r_k,d_2}}} y^{n_2} \right)^i \right. \\ & \times \left(\left(\frac{\delta_1^{\mathrm{th}} y}{\rho_r y - \varepsilon_1} \right)^{m_{g_{r_k,d_1}}-1} \exp\left(-\frac{\delta_1^{\mathrm{th}} y}{\beta_{g_{r_k,d_1}} (\rho_r y - \varepsilon_1)} \right) \right) \Bigg(dy. \end{aligned}$$

and

$$\begin{aligned}\Phi_2 =&1-F_{|g_{r_b,d_1}|^2}\left(\frac{\delta_1^{\text{th}}}{\rho_r}\right)\Bigg(\\ =&1-1-\frac{1}{\Gamma\left(m_{g_{r_b,d_1}}\right)}\Gamma\quad m_{g_{r_b,d_1}},\frac{\delta_1^{\text{th}}}{\rho_r\beta_{g_{r_b,d_1}}}\Bigg)\Bigg(\\ =&\frac{1}{\Gamma\left(m_{g_{r_b,d_1}}\right)}\Gamma\quad m_{g_{r_b,d_1}},\frac{\delta_1^{\text{th}}}{\rho_r\beta_{g_{r_b,d_1}}}\Bigg)\Bigg(\\ =&\mathrm{e}^{-\frac{\delta_1^{\text{th}}}{\rho_r\beta_{g_{r_k,d_1}}}}\sum_{n_3=0}^{m_{g_{r_k,d_1}}-1}\Bigg(\frac{\left(\delta_1^{\text{th}}\right)^{n_3}}{n_3!\rho_r^{n_3}\beta_{g_{r_k,d_1}}^{n_3}}.\end{aligned}\tag{66}$$

Substituting (66) and (66) into (60), η_1 can be computed.

Defining Ω_θ as the probability that the relay r_i is in the active relay set $\mathcal{B}_\mathcal{R}$, the Ω_θ can be mathematically formulated as

$$\begin{aligned}\Omega_\theta \triangleq&\Pr\left(r_i\in\mathcal{B}_\mathcal{R}\right)\\ =&\Pr\left\{|h_i|^2\geq\chi,|g_{r_b,d_1}|^2>\frac{\delta_1^{\text{th}}}{\rho_r}\right\}\Bigg(\\ =&\underbrace{\Pr\left\{|h_i|^2\geq\chi\right\}}_{\triangleq\varphi_1^*}\Bigg(\times\underbrace{\Pr\left\{|g_{r_b,d_1}|^2>\frac{\delta_1^{\text{th}}}{\rho_r}\right\}}_{\triangleq\varphi_2^*}\Bigg(\end{aligned}\tag{67}$$

We have

$$
\begin{aligned}
\varphi_1^* &= \Pr\left\{|h_i|^2 \geq \chi\right\} \\
&= \Pr\left\{|h_i|^2 \geq \frac{\mu}{\rho_s}\left(\rho_r|f_k|^2+1\right)\right\} \\
&= \int_0^\infty \left(1 - F_{|h_i|^2}\left(\frac{\mu}{\rho_s}\left(\rho_r x+1\right)\right)\right) f_{|f_k|^2}(x)\, dx \\
&= \int_0^\infty 1 - \left(1 - \exp\left(-\frac{\mu}{\beta_h\rho_s}\left(\rho_r x+1\right)\right)\sum_{n=0}^{m_h-1}\frac{\mu^n(\rho_r x+1)^n}{n!\rho_s^n\beta_h^n}\right)\frac{x^{m_{f_k}-1}}{\Gamma(m_{f_k})\,\beta_{f_k}^{m_{f_k}}}\exp\left(-\frac{x}{\beta_{f_k}}\right)dx \\
&= \exp\left(\frac{\mu}{\beta_h\rho_s}\right)\int_0^\infty \sum_{n=0}^{m_h-1}\frac{\mu^n(\rho_r x+1)^n}{n!\rho_s^n\beta_h^n}\frac{x^{m_{f_k}-1}}{\Gamma(m_{f_k})\,\beta_{f_k}^{m_{f_k}}}\exp\left(-\left(\frac{1}{\beta_{f_k}}+\frac{\mu\rho_r}{\beta_h\rho_s}\right)x\right)dx \\
&= \frac{\exp\left(-\mu/\beta_h\rho_s\right)}{\Gamma(m_{f_k})\,\beta_{f_k}^{m_{f_k}}}\int_0^\infty \sum_{n=0}^{m_h-1}\sum_{k=0}^{n}\binom{n}{k}\frac{\mu^n}{n!\rho_s^n\beta_h^n}x^{k+m_{f_k}-1}\exp\left(-\left(\frac{1}{\beta_{f_k}}+\frac{\mu\rho_r}{\beta_h\rho_s}\right)x\right)dx \\
&= \frac{\exp\left(-\mu/\beta_h\rho_s\right)}{\Gamma(m_{f_k})\,\beta_{f_k}^{m_{f_k}}}\sum_{n=0}^{m_h-1}\sum_{k=0}^{n}\binom{n}{k}\frac{\mu^n}{n!\rho_s^n\beta_h^n}\left(\frac{1}{\beta_{f_k}}+\frac{\mu\rho_r}{\beta_h\rho_s}\right)^{-k-m_{f_k}}\Gamma(k+m_{f_k}).
\end{aligned}
\tag{68}
$$

where $\mu = \max\left(\frac{\delta_1^{\text{th}}}{\upsilon_1-\upsilon_2\delta_1^{\text{th}}}, \frac{\delta_2^{\text{th}}}{\upsilon_2}\right)$, $\chi = \max\left(\frac{\delta_1^{\text{th}}}{\upsilon_1-\upsilon_2\delta_1^{\text{th}}}, \frac{\delta_2^{\text{th}}}{\upsilon_2}\right)\left(\frac{\rho_r|f_k|^2+1}{\rho_s}\right)$.
It is further to have φ_2^* computed by

$$
\begin{aligned}
\varphi_2^* &= 1 - F_{|g_{r_k,d_1}|^2}\left(\frac{\delta_1^{\text{th}}}{\rho_r}\right) \\
&= \frac{1}{\Gamma\left(m_{g_{r_k,d_1}}\right)}\Gamma\left(m_{g_{r_k,d_1}}, \frac{\delta_1^{\text{th}}}{\rho_r\beta_{g_{r_k,d_1}}}\right)
\end{aligned}
\tag{69}
$$

Then, the probability for the event that there are r_i active relays in $\mathcal{B}_\mathcal{R}$ can be evaluated as follows:

$$
\Pr\left(|\mathcal{B}_\mathcal{R}| = i\right) = \binom{M}{i}\left(\Omega_\theta\right)^i\left(1-\Omega_\theta\right)^{M-i}. \tag{70}
$$

Substituting result of (60) and (70) into (44), the outage probability of consideblack system can be computed as in Proposition 3. This completes the proof.

References

1. S. M. R. Islam et al., "Power-domain non-orthogonal multiple access (NOMA) in 5G systems: Potentials and challenges," IEEE Commun. Surveys Tuts., vol. 19, no. 2, pp. 721 - 742, 2017.

2. Z. Ding et al., "Application of NOMA in LTE and 5G networks," IEEE Commun. Mag., vol. 55, no. 2, pp. 185-191, 2017.
3. Z. Ding, "Cooperative non-orthogonal multiple access in 5G systems," IEEE Commun. Lett.,vol. 19, no. 8, pp. 1462-1465, 2015.
4. J. B. Kim et al., "NOMA in coordinated direct and relay transmission," IEEE Commun. Lett., vol. 19, no. 11, pp. 2037-2040, 2015.
5. J. Men et al.,"Performance analysis of non-orthogonal multiple access for relaying networks over Nakagami-m fading channels," IEEE Trans.Veh. Technol., vol. 66, no. 2, pp. 1200-1208, Feb. 2017.
6. Y. Li et al., "Performance analysis of cooperative NOMA with a shablack AF relay," IET Commun., vol. 12, no. 19, pp. 2438-2447, Nov. 2018.
7. K. Janghel et al., "Performance of adaptive OMA/cooperative-NOMA scheme with user selection," IEEE Commun. Lett., vol. 22, no. 10, pp. 1-1, Oct. 2018.
8. Dinh-Thuan Do and C.-B. Le, "Application of NOMA in Wireless System with Wireless Power Transfer Scheme: Outage and Ergodic Capacity Performance Analysis," Sensors, vol. 18, no. 10, p.3501, 2018.
9. T.-L. Nguyen and Dinh-Thuan Do, "Exploiting Impacts of Intercell Interference on SWIPT-assisted Non-orthogonal Multiple Access ," Wireless Communications and Mobile Computing, vol. 2018, Article ID 2525492, 12 pages , 2018.
10. Dinh-Thuan Do and M.-S. Van Nguyen, "Device-to-device transmission modes in NOMA network with and without Wireless Power Transfer," Computer Communications, Vol. 139, pp. 67-77, May 2019.
11. D.-T. Do, M. Vaezi and T.-L. Nguyen, "Wireless Poweblack Cooperative Relaying using NOMA with Imperfect CSI," in Proc. of IEEE Globecom Workshops (GC Wkshps), Abu Dhabi, UAE, pp. 1-6, 2018.
12. Z. Ding et al., "Relay selection for cooperative NOMA," IEEE Wirel. Commun. Lett., vol. 5, no. 4, pp. 416-419, Aug. 2016.
13. Z. Yang et al., "Novel RS strategies for cooperative NOMA," IEEE Trans. Veh. Technol., vol. 66, no. 11, pp. 10 114-10 123, Sept. 2017.
14. P. Xu et al., "Optimal relay selection schemes for cooperative NOMA," IEEE Trans. Veh. Technol., vol. 67, no. 8, pp. 7851-7855, Aug. 2018.
15. Dinh-Thuan Do, M.-S. Van Nguyen, T.-A. Hoang and M. Voznak, "NOMA-Assisted Multiple Access Scheme for IoT Deployment: Relay Selection Model and Secrecy Performance Improvement," Sensors, vol. 19, no. 3, p. 736, 2019.
16. A. Bletsas, A. Khisti, D. Reed and A. Lippman, "A simple cooperative diversity method based on network path selection," IEEE J. Select. Areas Commun., vol. 24, pp. 659-672, March 2006.
17. D. S. Michalopoulos and G. K. Karagiannidis, "Performance analysis of single relay selection in Rayleigh fading," IEEE Trans. Wireless Commun., vol. 7, pp. 3718-3724, Oct. 2008.
18. N. Nomikos, T. Charalambous, I. Krikidis, D. N. Skoutas, D. Vouyioukas, M. Johansson, C. Skianis, "A survey on buffer-aided relay selection," IEEE Commun. Surv. and Tut., vol. 18, no. 2, pp. 1073-1097, Secondquarter 2016.
19. N. Zlatanov, A. Ikhlef, T. Islam and R. Schober, "Buffer-aided cooperative communications: opportunities and challenges," IEEE Commun. Mag. , vol. 52, no. 4, pp. 146-153, April 2014.
20. A. Ikhlef, D. S. Michalopoulos and R. Schober, "Max-max relay selection for relays with buffers," IEEE Trans. Wireless Commun., vol. 11, pp. 1124-1135, March 2012.
21. I. Krikidis, T. Charalambous and J. S. Thompson, "Buffer-aided relay selection for cooperative diversity systems without delay constraints," IEEE Trans. Wireless Commun., vol. 11, pp. 1957-1967, May 2012.
22. M. Oiwa, C. Tosa and S. Sugiura, "Theoretical analysis of hybrid buffer-aided cooperative protocol based on max?max and max?link relay selections," IEEE Trans. on Vehic. Tech., vol. 65, no. 11, pp. 9236-9246, Nov. 2016.
23. D. Poulimeneas, T. Charalambous, N. Nomikos, I. Krikidis, D. Vouyioukas, M. Johansson, "A delay-aware hybrid relay selection policy," IEEE Int. Conf. on Telecomm., (ICT), May 2016.

24. Z. Tian, Y. Gong, G. Chen and J. Chambers, "Buffer-aided relay selection with blackuced packet delay in cooperative networks," IEEE Trans on Vehic. Tech., vol. 66, no. 3, pp. 2567-2575, March 2017.
25. S. Luo and K. C. Teh, "Buffer state based relay selection for buffer-aided cooperative relaying systems," IEEE Trans. on Wireless Commun., vol. 14, no. 10, pp. 5430-5439, Oct. 2015.
26. N. Nomikos, D. Poulimeneas, T. Charalambous, I. Krikidis, D. Vouyioukas and M. Johansson, "Delay- and diversity-aware buffer-aided relay selection policies in cooperative networks," IEEE Access, Nov. 2018.
27. S. L. Lin and K. H. Liu, "Relay selection for cooperative relaying networks with small buffers," IEEE Trans. on Vehic. Tech., vol. 65, no. 8, pp. 6562-6572, Aug. 2016.
28. W. Wicke, N. Zlatanov, V. Jamali and R. Schober, "Buffer-aided relaying with discrete transmission rates for the two-hop half-duplex relay network," IEEE Trans. on Wireless Commun., vol. 16, no. 2, pp. 967-981, Feb. 2017.
29. B. Zhou, Y. Cui and M. Tao, "Stochastic throughput optimization for two-hop systems with finite relay buffers," IEEE Trans. on Signal Proc., vol. 63, no. 20, pp. 5546-5560, Oct. 2015.
30. M. Oiwa; R. Nakai; S. Sugiura, "Buffer-state-and-thresholding-based amplify-and-forward cooperative networks," IEEE Wireless Commun. Lett., vol. 6, no. 5, pp. 674-677, Oct. 2017.
31. D. Kim, H. Lee, and D. Hong, "A survey of in-band full-duplex transmission: From the perspective of PHY and MAC layers," IEEE Commun. Surveys Tuts., vol. 17, no. 4, pp. 2017-2046, Fourth Quarter 2015.
32. M. Jain, J. I. Choi, T. Kim, D. Bharadia, S. Seth, K. Srinivasan, P. Levis, S. Katti, and P. Sinha, "Practical, real-time, full duplex wireless," in Proc. ACM MobiCom, Las Vegas, NV, Sept. 2011.
33. W. Li, J. Lilleberg, and K. Rikkinen, "On rate region analysis of half-and full-duplex OFDM communication links," IEEE J. Sel. Areas Commun., vol. 32, no. 9, pp. 1688-1698, Sept. 2014.
34. A. Tregancini, E. E. B. Olivo, D. P. M. Osorio, C. H. M. de Lima and H. Alves, "Performance Analysis of Full-Duplex Relay-Aided NOMA Systems Using Partial Relay Selection," in IEEE Transactions on Vehicular Technology, vol. 69, no. 1, pp. 622-635, Jan. 2020.
35. H. Dang, M. Van Nguyen, D. Do, H. Pham, B. Selim and G. Kaddoum, "Joint Relay Selection, Full-Duplex and Device-to-Device Transmission in Wireless Powered NOMA Networks," in IEEE Access, vol. 8, pp. 82442-82460, 2020.
36. N. Nomikos, T. Charalambous, D. Vouyioukas, R. Wichman and G. K. Karagiannidis, "Integrating Broadcasting and NOMA in Full-Duplex Buffer-Aided Opportunistic Relay Networks," in IEEE Transactions on Vehicular Technology, vol. 69, no. 8, pp. 9157-9162, Aug. 2020.
37. J. Zhao, Z. Ding, P. Fan, Z. Yang, and G. K. Karagiannidis, "Dual Relay Selection for Cooperative NOMA With Distributed Space Time Coding," IEEE Access, vol. 6, pp. 20440-20450, 2018.
38. Seventh Edition , "Table of Integrals, Series, and Products", 2007.
39. Z. Ding, H. Dai, H. V. Poor, "Relay Selection for Cooperative NOMA," IEEE Wireless Communications Letters, vol. 5, no. 4, pp. 416-419, 2016.
40. Z. Xiang, W. Yang, Y. Cai, J. Xiong, Z. Ding and Y. Song, "Secure Transmission in a NOMA-Assisted IoT Network With Diversified Communication Requirements," in IEEE Internet of Things Journal, vol. 7, no. 11, pp. 11157-11169, Nov. 2020, doi: 10.1109/JIOT.2020.2995609.